ASYMPTOTIC RESULTS FOR BIFURCATIONS IN PURE BENDING OF RUBBER BLOCKS

by CIPRIAN D. COMAN†

(*Department of Mathematics, University of Glasgow,* 15 *University Gardens, Glasgow* G12 8QW, *United Kingdom*)

and

MICHEL DESTRADE

(*Institut Jean Le Rond d'Alembert, Centre National de la Recherche Scientifique (CNRS)/Université Pierré et Marie Curie, Case* 162, 75252 *Paris Cedex* 05, *France*)

[Received 28 November 2007. Revise 22 February 2008. Accepted 7 March 2008]

Summary

The bifurcation of an incompressible neo-Hookean thick block with a ratio of thickness to length η, subject to pure bending, is considered. The two incremental equilibrium equations corresponding to a nonlinear pre-buckling state of strain are reduced to a fourth-order linear eigenproblem that displays a multiple turning point. It is found that for $0 < \eta < \infty$, the block experiences an Euler-type buckling instability which in the limit $\eta \to \infty$ degenerates into a surface instability. Singular perturbation methods enable us to capture this transition, while direct numerical simulations corroborate the analytical results.

1. Introduction

The development of compressive stresses in mechanical structures is well known to be responsible for Euler-type buckling instabilities. What is less recognised is that such scenarios are likely to occur in a number of cases that, apparently, are of a completely different nature. A typical example is the phenomenon of stress concentration in perforated thin elastic plates subjected to tension. Usually, the holes act as stress concentrators that can be completely or only partially surrounded by compressed regions. If the pulling forces are sufficiently strong, an out-of-plane bending instability is experienced locally near the sites of the holes. A systematic investigation of problems of this nature has recently been initiated by Coman *et al.* (**1** to **3**).

A second example where Euler-type buckling is indirectly encountered is provided by the pure bending of a thin and short elastic tube. The curved configuration adopted by the tube is characterised by compressive axial stresses on the concave side, whereas tension prevails on the convex part. Experience shows that a regular instability pattern consisting of many little ripples will develop along the former region, eventually leading to the creation of one or several kinks that signal the collapse of the tube.

The stability problem of pure bending in thin-walled tubular structures has a long history and there is a vast mechanical engineering literature dealing with various aspects; some of it is aptly summarised in the authoritative monograph by Kyriakides and Corona (**4**). On the mathematical

†⟨cdc@maths.gla.ac.uk⟩

Q. Jl Mech. Appl. Math, Vol. 61. No. 3
Advance Access publication 16 April 2008. doi:10.1093/qjmam/hbn009

side, noteworthy contributions in the present context are the works by Seide and Weingarten (**5**) and Tovstik and Smirnov (briefly summarised in (**6**)). The former investigation is based on the Donnell-von Kármán buckling equations linearised around a variable-coefficient membrane state of stress. The resulting boundary-value problem was analysed numerically with the help of the Galerkin method, and it was found that the circumferential shape of the buckled cylinder displays a small dimple on the compressed side. Several versions of the same problem have been reconsidered in (**6**) from the point of view of asymptotic analysis. Both works just now mentioned made the simplifying assumption that the rippling pattern is the same at every point along the axis of the cylinder or, in other words, a solution with separable variables was *a priori* postulated. The assumption is sensible for short tubes (which are fairly stiff), but it is inadequate for modelling the collapse in the elastoplastic regime for moderate lengths, which turns out to require a very different approach (cf. (**4**)).

Our main aim in the present investigation is to revisit the pure bending of a rubber block deforming in plane strain, a problem that has several points in common with the tube bending mentioned above. Unfortunately, the literature in this area has focussed mainly on describing the deformation itself rather than its potential bifurcations. The typical scenario is outlined in Fig. 1: the undeformed configuration is shown in the left-hand sketch and is characterised by the geometric parameters $2L$ (length), H (height) and $2A$ (thickness); the deformed block appears in the same figure, on the right. The plane strain hypothesis simplifies the problem considerably, since one needs to deal only with cross sections (shown shaded) perpendicular to the vertical axis of the block and situated sufficiently far away from the lower and upper faces.

Pioneering work on pure bending stability was carried out by Triantafyllidis (**7**), who examined incremental bifurcation equations for a couple of piecewise power-law constitutive models, including a hypoelastic one. He pointed out that the underlying instability mechanism is a surface instability similar to that encountered in the plane strain half-space problems discussed by Hill and Hutchinson (**8**) or Young (**9**). Haughton (**10**) performed a similar analysis for hyperelastic materials in a three-dimensional context (neo-Hookean, mostly) and allowed for vertical compression as well. The instability was found to be of Euler type but his interpretation of some of the results can

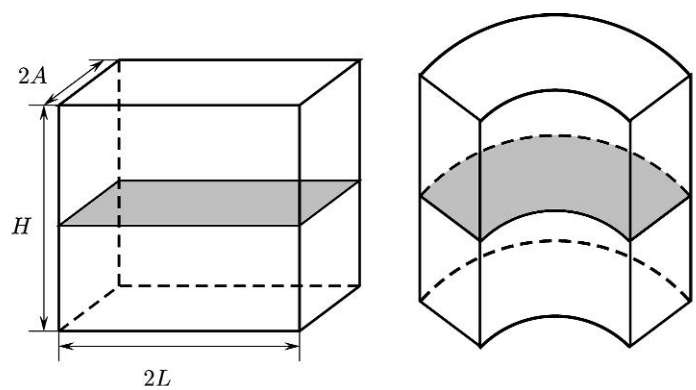

Fig. 1 Cylindrical bending of a rubber block; *left*: reference configuration, *right*: current configuration. Shaded areas indicate two generic cross sections perpendicular to the vertical axis

be improved upon, as we explain in section 3. A novel feature in (**10**) is the interaction between two different modes of instability, one due to pure bending and the other related to compression. Dryburgh and Ogden (**11**) introduced thin coatings on the curved boundaries of the bent block and made comparisons with the uncoated case. Their findings show that, relative to the latter case, bifurcation is generally promoted by the presence of surface coating, on either or both curved boundaries, that is, the bifurcation occurs at smaller strains. The relative sizes of the shear moduli for the coating and, respectively, the bulk material were found to play an important role in describing this phenomenon.

The finite elasticity works reviewed above share a common feature in that they all deal with incompressible materials. So far, little is known about the role played by compressibility on the bifurcation behaviour in pure bending. The reason might be rooted in the absence from the literature of a manageable closed-form expression for the pre-bifurcation deformation. Aron and Wang (**12**, **13**) touched upon issues like existence and uniqueness for bending deformations in unconstrained elastic materials, while Bruhns *et al.* (**14**) used Hencky's compressible elasticity model to investigate closed-form solutions for cylindrical bending. They succeeded in deriving explicit expressions for the bending angle and moment in terms of the circumferential stretches on the curved boundaries. The solution is quite involved and it seems unlikely to be useful for anything but numerical calculations. Moreover, the particular Hencky's elasticity framework is restricted to moderate deformations only.

A critique of bifurcation phenomena in pure bending was given by Gent and Cho (**15**) who pointed out that their experiments did not agree with the theoretical predictions based on the surface instability concept proposed in (**7**). In particular, they found that the instability occurs for a smaller degree of compression and the block adopts a configuration with a small number of sharp creases on the inner surface. To fully explain this observation would require a nonlinear post-buckling analysis because the bifurcation involved is probably of subcritical type. We note in passing that Gent and Cho's creases are, to a certain extent, very similar to those encountered on the curved surface of severely torsioned stocky rubber cylinders (**16**). These phenomena are likely to be related to the failure at the boundary of the complementing condition (see (**17**) and the references therein), and they fall outside the scope of our study.

With this background in mind, we reconsider in the next sections a particular instance of the pure bending problems taken up in (**10**, **11**). The aim is to elucidate the nature of the instability and to analyse the mathematical structure of the governing boundary-value problem when $\eta \equiv A/L \gg 1$. To reduce the algebraic complexity of the bifurcation equations, we focus on the incompressible neo-Hookean elastic material. In section 2, these assumptions are shown to yield an eigenproblem for a fourth-order partial differential equation with variable coefficients, subsequently simplified by seeking a solution with separable variables. Direct numerical simulations reveal an Euler-type buckling phenomenon for $0 < \eta < \infty$, but in the limit $\eta \to \infty$ this degenerates into a surface instability. Some erroneous interpretations proposed by previous investigators (for example, (**7**) or (**10**)) are also corrected here for the first time. As demonstrated in section 4, the transition regime between the two different forms of instabilities can be efficiently captured by singular perturbation methods. The two contrasting asymptotic methods employed are discussed separately in sections 4.1 (WKB analysis) and 4.2 (boundary-layer (BL) approach), respectively. The former would seem to be the most appropriate because the differential equation in question has variable coefficients. However, it transpires that conventional BL arguments shed more light and help us to steer clear from the confusion created by the presence of a multiple turning point. Unlike the recent asymptotic studies (**1** to **3**), here turning points play no role whatsoever (the same assertion appears to hold for the related works (**18**, **19**)). The paper concludes with a discussion of the results obtained, together with suggestions for further study.

2. Overview of the model

Finite pure bending of incompressible hyperelastic materials is discussed in a number of books such as (**20**) or (**21**), for example. To make the paper reasonably self-contained, we summarise some of those ideas below.

The reference configuration of the initially undeformed rectangular cross section of the hyperelastic block is the region (see Fig. 2)

$$\mathcal{B}_{\mathrm{R}} := \{(X_1, X_2) \in \mathbb{R}^2 \mid -A \leqslant X_1 \leqslant A, -L \leqslant X_2 \leqslant L\}.$$

Supposing that the block is bent (symmetrically with respect to the x_1-axis) into a sector of circular cylindrical tube, the current configuration of the deformed cross section is easily represented in polar coordinates by the domain

$$\mathcal{B}_{\mathrm{C}} := \{(r, \theta) \in \mathbb{R} \times (-\pi, \pi] \mid r_1 \leqslant r \leqslant r_2, -\omega_0 \leqslant \theta \leqslant \omega_0\}.$$

Rivlin (**22**) showed that for an incompressible elastic material, this type of deformation may be described by the mapping

$$r = (d + 2X_1/\omega)^{1/2}, \quad \theta = \omega X_2, \tag{2.1}$$

where d is a quantity to be specified later and ω can serve as a control parameter as it is related to the angle of bending, $\omega_0 := \omega L$. Since the plate cannot be bent into itself, we require that

$$0 \leqslant \omega_0 < \pi, \tag{2.2}$$

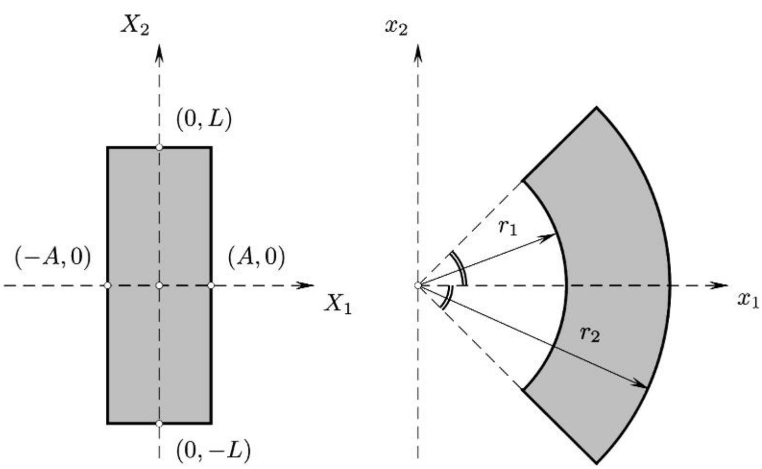

Fig. 2 The undeformed (left) and deformed (right) cross sections of the rubber block shown in Fig. 1. Bending is symmetric with respect to the x_1-axis so that the two angles marked are congruent and equal to ω_0; see the text for more details

an assumption used tacitly henceforth. Although the deformation recorded in (2.1) seems to have an iconic status among workers in finite elasticity, it is clear that the kinematics afforded by that expression are somewhat restricted. The lines $X_1 =$ constant become arcs of the circle $r =$ constant, while the lines $X_2 =$ constant are transformed in lines $\theta =$ constant; in other words, 'cross sections' perpendicular to the vertical symmetry axis of $\mathcal{B}_{\mathrm{R}}$ remain orthogonal to the deformed axis of the current configuration $\mathcal{B}_{\mathrm{C}}$. This is somewhat at odds with the commonly accepted point of view in structural mechanics, according to which pure bending of thick sandwich panels (for example, (**23**)) is based on models that allow cross sections to slide relative to the normal to the deformed axis. Nonetheless, the nonlinear mapping (2.1) is still a sensible choice for the type of questions we want to answer, at least in a first approximation.

The bifurcation analysis carried out in this work is based upon linearising the plane strain equations of finite elasticity around the nonlinear pre-buckling deformation (2.1). This approach to linearised, or incremental, bifurcations is well established (see (**21**, **24**), for example), so we shall not rehearse it here. Instead, we limit ourselves to pointing out the key steps that lead to our eigenproblem.

We assume that the constitutive behaviour of the material is characterised by a strain energy function $W \equiv W(\lambda_r, \lambda_\theta)$, where the principal stretches λ_r and λ_θ are associated with the Eulerian principal directions $\mathbf{e}_r$ and, respectively, $\mathbf{e}_\theta$. Due to the incompressibility constraint, these can be written as

$$\lambda_r = \lambda^{-1} \quad \text{and} \quad \lambda_\theta \equiv \lambda := \omega r,$$

which defines the notation λ. According to Ogden (**21**), the two-dimensional version of the incremental equations of equilibrium for incompressible elasticity reads

$$\operatorname{div} \mathring{\mathbf{s}} = \mathbf{0} \quad \text{and} \quad \operatorname{div} \mathring{\mathbf{u}} = 0, \tag{2.3}$$

where $\mathring{\mathbf{u}} = (\mathring{u}(r,\theta), \mathring{v}(r,\theta))$ is the incremental displacement field and $\mathring{\mathbf{s}}$ denotes the incremental nominal stress tensor with components

$$\mathring{s}_{ij} = L_{ijkl}\mathring{F}_{kl} + p\mathring{F}_{ij} - \mathring{p}\delta_{ij}, \quad i, j \in \{r, \theta\}.$$

Here, $\mathring{p}$ is the increment in the Lagrange multiplier $p \equiv p(r,\theta)$ associated with the internal constraint of incompressibility and $\mathring{F}_{ij}$ represent the components of the incremental deformation gradient

$$\mathring{\mathbf{F}} = \begin{bmatrix} \mathring{u},_r & \frac{1}{r}(\mathring{u},_\theta - \mathring{v}) \\ \mathring{v},_r & \frac{1}{r}(\mathring{u} + \mathring{v},_\theta) \end{bmatrix}.$$

Finally, L_{ijkl} are the components of the fourth-order tensor of instantaneous incremental moduli which, in Eulerian principal axes, has six independent non-zero such components (cf. (**21**))

$$L_{iijj} = \lambda_i \lambda_j W_{ij}, \tag{2.4a}$$

$$L_{ijij} = \begin{cases} \dfrac{\lambda_i^2(\lambda_i W_i - \lambda_j W_j)}{\lambda_i^2 - \lambda_j^2}, & \text{if } i \neq j, \lambda_i \neq \lambda_j, \\ \frac{1}{2}(L_{iiii} - L_{iijj} + \lambda_i W_i), & \text{if } i \neq j, \lambda_i = \lambda_j, \end{cases} \tag{2.4b}$$

$$L_{ijji} = L_{jiij} = L_{ijij} - \lambda_i W_i, \tag{2.4c}$$

where $W_i \equiv \partial W / \partial \lambda_i$, $W_{ij} \equiv \partial^2 W / \partial \lambda_i \partial \lambda_j$ and the summation convention does not apply.

Direct calculations show that the system of equations (2.3) can be reduced to

$$r^2\mathring{p}_{,r} = r[r(L'_{1111} - L'_{1122} + p_{,r}) + L_{1111} + L_{2222} - 2L_{1122}]\mathring{u}_{,r} + r^2(L_{1111} - L_{1122})\mathring{u}_{,rr} + L_{2121}(\mathring{u}_{,\theta\theta} - \mathring{v}_{,\theta}) + rL_{2112}\mathring{v}_{,r\theta}, \tag{2.5}$$

$$r\mathring{p}_{,\theta} = (rL'_{1212} + L_{1212})(r\mathring{v}_{,r} + \mathring{u}_{,\theta} - \mathring{v}) + r^2L_{1212}\mathring{v}_{,rr} + r(L_{2112} + L_{1122} - L_{2222})\mathring{u}_{,r\theta}. \tag{2.6}$$

To avoid overloading the notation, we used the correspondence $r \to 1$ and $\theta \to 2$ for the incremental moduli, and we indicated their derivatives with respect to r by dashes. A further simplification is afforded by the incremental incompressibility condition in (2.3), which allows us to deduce the existence of a potential $\phi \equiv \phi(r, \theta)$ such that

$$\mathring{u} = \frac{1}{r}\frac{\partial\phi}{\partial\theta} \quad \text{and} \quad \mathring{v} = -\frac{\partial\phi}{\partial r}. \tag{2.7}$$

The upshot of this observation is that the two equations (2.5) and (2.6) can now be combined into a single partial differential equation for the potential function. After some routine (but lengthy) manipulations, we get

$$\sum_{j=1}^{4}\mathcal{L}_j[\phi] = 0, \tag{2.8}$$

with $\mathcal{L}_j$, partial differential operator of the jth order, defined according to

$$\mathcal{L}_4 := \alpha r^4\frac{\partial^4}{\partial r^4} + 2\beta r^2\frac{\partial^4}{\partial r^2\partial\theta^2} + \gamma\frac{\partial^4}{\partial\theta^4},$$

$$\mathcal{L}_3 := 2r^3(r\alpha)'\frac{\partial^3}{\partial r^3} + 2r^3\left(\frac{\beta}{r}\right)'\frac{\partial^3}{\partial r\partial\theta^2},$$

$$\mathcal{L}_2 := r^4\left[\alpha'' + \left(\frac{\alpha}{r}\right)'\right]\frac{\partial^2}{\partial r^2} - r^2\left[\alpha'' + \left(\frac{\alpha + 2\beta}{r}\right)' - \frac{\gamma}{r^2}\right]\frac{\partial^2}{\partial\theta^2},$$

$$\mathcal{L}_1 := -r^3\left[\alpha'' + \left(\frac{\alpha}{r}\right)'\right]\frac{\partial}{\partial r},$$

and

$$\alpha(r) := L_{1212}, \quad \gamma(r) := L_{2121}, \quad \beta(r) := \frac{1}{2}(L_{1111} + L_{2222}) - (L_{1122} + L_{2112}).$$

The form (2.8) of the bifurcation equation is valid for any choice of incompressible hyperelastic material but, as it stands, the model is not easily amenable to analytical work. Before further simplifications are implemented, we must address the issue of boundary conditions.

The two curved boundaries of $\mathcal{B}_C$ are assumed to be free of incremental tractions

$$\alpha r^3\phi_{,rrr} - (2\beta + \alpha)(\phi_{,\theta\theta} - r\phi_{,r\theta\theta}) = 0, \quad \text{for } (r, \theta) \in \{r_1, r_2\} \times (-\pi, \pi], \tag{2.9a}$$

$$\phi_{,\theta\theta} + r\phi_{,r} - r^2\phi_{,rr} = 0, \quad \text{for } (r, \theta) \in \{r_1, r_2\} \times (-\pi, \pi]; \tag{2.9b}$$

these conditions can be obtained as a particular case of the calculations of Dryburgh and Ogden (**11**), to which the reader is referred for more information.

Next, we look for separable solutions of the bifurcation equation (2.8) in the form

$$\phi(r, \theta) = \Phi(r)\cos(m\theta), \tag{2.10}$$

where $m \in \mathbb{N}$ is the azimuthal mode number related to the number of ripples on the compressed side of the rubber block, while $\Phi(r)$ represents the infinitesimal amplitude of this cosine rippling pattern. Several types of boundary conditions are possible for the straight boundaries of $\mathcal{B}_{\mathrm{C}}$. Following Haughton (**10**) and Dryburgh and Ogden (**11**), we consider zero incremental displacement in the radial direction and vanishing normal traction. It can be shown that these conditions are satisfied as long as

$$m = \frac{n\pi}{\omega L} \equiv \frac{n\pi}{\omega_0}, \tag{2.11}$$

for some positive $n \in \mathbb{Z}$. With this information in hand, all that remains to be done is to choose a constitutive model and carry out the simplification of (2.8) with the help of the assumed form solution recorded in (2.10).

The bulk material is modelled by a simple neo-Hookean strain energy function specialised to plane strain elasticity

$$W(\lambda_r, \lambda_\theta) = \frac{1}{2}\tau(\lambda_r^2 + \lambda_\theta^2 - 2),$$

τ being the shear modulus of the material. (In fact, the analysis conducted henceforth also applies to the Mooney–Rivlin material, which coincides with the neo-Hookean material in plane strain.) As shown by Rivlin (**22**) and subsequently discussed by others (**7**, **10**, **11**), for this particular choice of constitutive law the constant d in (2.1) is determined by

$$d = \frac{L^2}{\omega_0^2}(1 + 4\eta^2\omega_0^2)^{1/2}.$$

On making use of (2.10) in (2.8) results in a fourth-order ordinary differential equation. When expressed in terms of the non-dimensional variables ρ (radius), μ (related to the mode number) and η (aspect ratio), defined by

$$\rho := \frac{r}{L}, \quad \mu := n\pi, \quad \eta := \frac{A}{L},$$

it can be cast as

$$\Phi'''' + \mathcal{P}(\rho)\Phi''' + \mathcal{Q}(\rho)\Phi'' + \mathcal{R}(\rho)\Phi' + \mathcal{S}(\rho)\Phi = 0, \quad \text{on } \rho_1 < \rho < \rho_2. \tag{2.12}$$

Above, the dashes denote derivatives with respect to ρ and

$$\mathcal{P}(\rho) := -\frac{2}{\rho}, \qquad \mathcal{Q}(\rho) := \left[\frac{3}{\rho^2} - \mu^2\left(\omega_0^2\rho^2 + \frac{1}{\omega_0^2\rho^2}\right)\right],$$

$$\mathcal{R}(\rho) := -\frac{1}{\rho}\left[\frac{3}{\rho^2} + \mu^2\left(\omega_0^2\rho^2 - \frac{3}{\omega_0^2\rho^2}\right)\right], \quad \mathcal{S}(\rho) := \mu^4.$$

Note that the inner and, respectively, the outer curved surfaces of the current configuration become

$$\rho_{1,2} = \frac{1}{\omega_0}[(1 + 4\eta^2\omega_0^2)^{1/2} \pm 2\eta\omega_0]^{1/2}, \tag{2.13}$$

while the principal stretch in the $\mathbf{e}_\theta$-direction assumes the simple form

$$\lambda = \omega_0 \rho. \tag{2.14}$$

The solution of (2.12) is found subject to the non-dimensional boundary conditions obtained from (2.9) via (2.10):

$$\Phi''' - \mu^2 \left(\omega_0^2 \rho^2 + \frac{2}{\omega_0^2 \rho^2} \right) \Phi' + \frac{\mu^2}{\rho} \left(\omega_0^2 \rho^2 + \frac{2}{\omega_0^2 \rho^2} \right) \Phi = 0, \quad \text{for } \rho = \rho_{1,2}, \tag{2.15a}$$

$$\Phi'' - \frac{1}{\rho}\Phi' + \frac{\mu^2}{\omega_0^2 \rho^2}\Phi = 0, \quad \text{for } \rho = \rho_{1,2}. \tag{2.15b}$$

Now, the normal mode approach has reduced the bifurcation analysis to the study of a standard ordinary eigenproblem for $\Phi(\rho)$ and $\omega_0 \in (0, \pi)$. The shear modulus of the neo-Hookean solid plays no role in the eigenproblem: in that sense, the nonlinear effects are purely geometrical. For structural mechanics problems (for example, (**25**)), the route taken above is free of pitfalls, whereas in finite elasticity it is only deceptively so. The danger is that the bent block might develop shear bands or other material instabilities before the compressed inner surface starts to wrinkle. Such occurrences are heralded by a loss of ellipticity in the partial differential equation (2.8); unfortunately, they remain undetected by (2.12). Conveniently, the use of a neo-Hookean constitutive law precludes any form of material instabilities (note that $\mathcal{L}_4$ is strongly elliptic in this case). Such exotic effects, however, were accounted for in (**7**), but it was found that the "surface instability" was always the first to occur.

3. Numerical experiments

The stability of the bent rubber block is now investigated numerically, the starting point being the eigenproblem (2.12), (2.15) formulated in section 2. Our first objective is to find out the dependence of the critical bending angle ω_0 on the aspect ratio $\eta \equiv A/L$. It is expected that an Euler-type buckling instability is experienced for $0 < \eta < \infty$ but that in the limit $\eta \to \infty$, this behaviour degenerates into a surface instability. Such behaviour is consistent with the results of Haughton (**10**) and Dryburgh and Ogden (**11**). It appears that earlier investigators (**7**, **15**) reported only surface instabilities although intuitively one would expect that the finite thickness of the block should set a length scale for the deformation pattern (recall that there is no characteristic length in surface instability problems).

A peculiar feature of our eigenproblem is the dependence of the mode number m in (2.11) on the bending angle ω_0. In order to identify the former quantity for a given η, we plot the critical principal stretch on the curved inner boundary $\rho = \rho_1$ in terms of this number, the critical value of m being that associated with the largest $\lambda_1 \equiv \lambda(\rho_1; \eta, n)$ when $n \in \mathbb{N}$. The practical implementation of the procedure is reported in Fig. 3, where we consider a sample of values for η (see the caption for details): the horizontal axis records the mode number n/ω_0, while the vertical axis shows λ_1. Strictly speaking, $n \in \mathbb{N}$ but here we take this parameter to be a positive real number ($\geqslant 1$) and note that ω_0, the eigenvalue of the problem (2.12), (2.15), depends on this quantity as well as on η, that is, $\omega_0 \equiv \omega_0(\eta, n)$. For $\eta = 1$, we find the curve shown with a continuous line and which consists of two sloping parts separated by a peak, P_1 (corresponding to $n \simeq 2{\cdot}43$). Henceforth, we refer to this curve as $\mathcal{C}_1$. Note that the right-hand part is monotonic decreasing

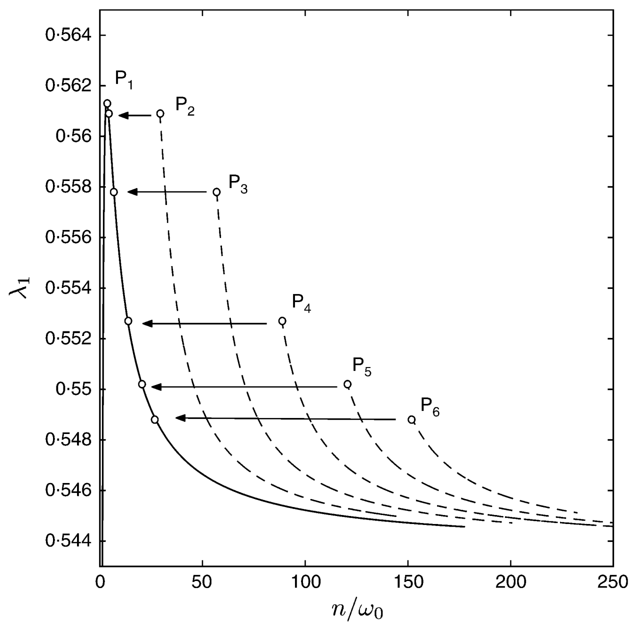

Fig. 3 Plot of the critical stretch $\lambda_1 \equiv \lambda(\rho_1)$ against $m/\pi \equiv n/\omega_0$, as obtained by direct numerical integration of the eigenproblem (2.12), (2.15) for a sample of aspect ratios η. The maximum principal stretch for each individual case considered is marked by a small circle and corresponds to the points P_1 ($\eta = 1{\cdot}0$), P_2 ($\eta = 3{\cdot}0$), P_3 ($\eta = 5{\cdot}0$), P_4 ($\eta = 10{\cdot}0$), P_5 ($\eta = 15{\cdot}0$) and P_6 ($\eta = 20{\cdot}0$). These maxima are attained for $n = 1$, except for P_1 that corresponds to $n \simeq 2{\cdot}43$

and unbounded but here only a segment of that curve is shown. The neutral stability curves for the other values of $\eta = \eta_j > 1$ considered are $\mathcal{C}_j := \{(\lambda_1(\rho_1; \eta_j, n), n/\omega_0)\,|\, n \in \mathbb{R}_+, n \geqslant 1\}$, and they all turn out to be part of $\mathcal{C}_1$. (As pointed out by an anonymous referee, this is best seen by rescaling (2.12), (2.15) with the help of the new independent variable $Z := \rho\omega_0$ and the parameter $\widehat{\mu} := \mu/\omega_0$; the resulting eigenvalue problem for $\Phi(Z)$ involves now only λ_1 and m.) The remark made above regarding $\mathcal{C}_1$ applies to the $\mathcal{C}_j$ curves as well. For the sake of clarity in Fig. 3, the curves are shifted to the right by equal amounts and shown separately as dashed lines, but their top end points ($P_2 - P_6$) are marked on $\mathcal{C}_1$ as well. All such points correspond to the choice $n = 1$.

The feature illustrated in Fig. 3 is generic and not restricted to the particular values of $\eta > 1$ chosen. A first observation is that the number of ripples on the compressed side of the block increases with the non-dimensional thickness η. When this latter quantity is reasonably large ($\eta \gtrsim 3$), the critical mode number given by (2.11) always corresponds to $n = 1$. Thus, the behaviour of a very thick block can be understood in two different ways: (i) assuming that $n = 1$ and $\eta \gg 1$ or, conversely, (ii) fixing $\eta = \mathcal{O}(1)$ and letting $n \gg 1$.

It is instructive to gain some insight into the behaviour of the critical eigenfunctions associated with the P_j's marked on Fig. 3. This information is included in Fig. 4, where we show the radial and azimuthal displacements only for $P_1 - P_4$, as obtained from the two equations in (2.7). The

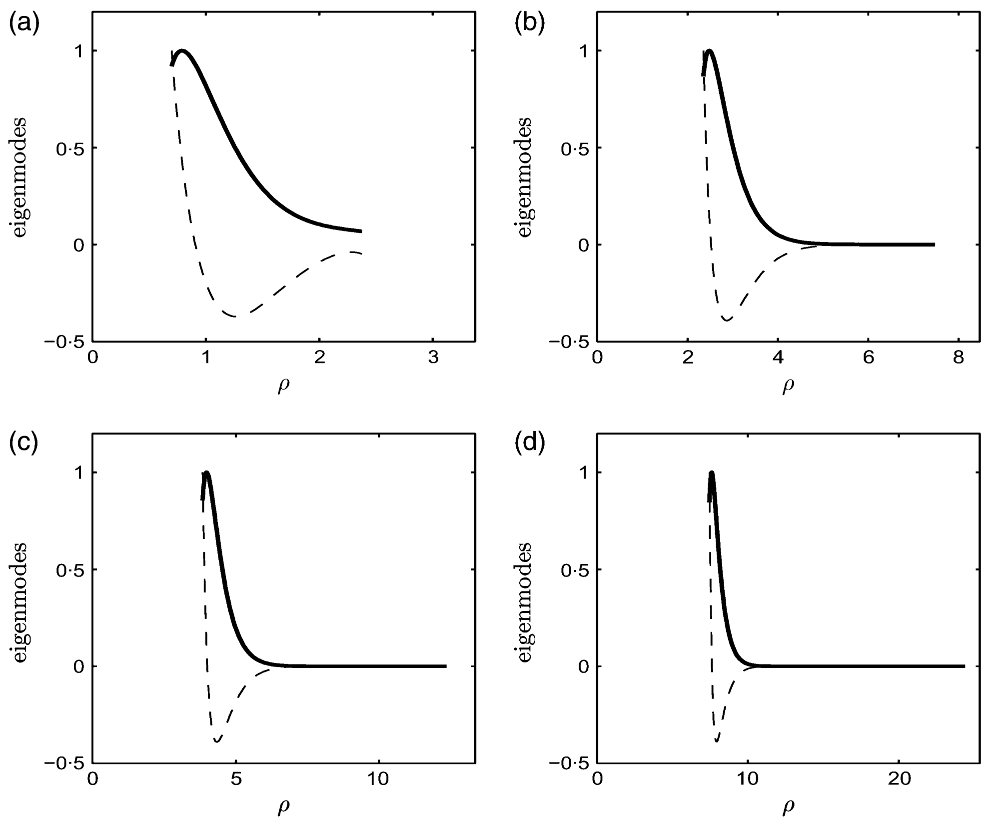

Fig. 4 The eigenfunctions associated with the critical points P_j in Fig. 3: (a) P_1 ($\eta = 1{\cdot}0$), (b) P_2 ($\eta = 3{\cdot}0$), (c) P_3 ($\eta = 5{\cdot}0$) and (d) P_4 ($\eta = 10{\cdot}0$). In each plot, the continuous line represents $\rho^{-1}\Phi(\rho)$ (radial displacement) and the dashed line is the graph of $\Phi'(\rho)$ (azimuthal displacement). The range for these functions is $\rho_1 \leqslant \rho \leqslant \rho_2$ and they are suitably normalised so that their maximum amplitude is unity

localisation of the deformation near the curved inner surface of the bent block when η increases is clear. The stress concentration phenomenon revealed by these plots is to be expected because the thicker the rubber block, the more difficult it is to bend, that is, the instability is likely to occur for small values of the bending angle. Hence, curvature effects are only 'felt' in the immediate proximity of the bent inner surface. In the remainder of the paper, we show that this behaviour is ideally suited for a singular perturbation analysis.

At this juncture, some remarks on the method used to identify the critical mode number are appropriate. At first sight, our work in Fig. 3 might appear a bit long winded. The coincidence of the curves $\mathcal{C}_j$ ($j = 2, \ldots, 6$) with $\mathcal{C}_1$ could have been inferred by taking into account that the principal stretch λ_1 is independent of n and depends only on the product $\omega_0\eta$—see (2.13) and (2.14). However, we believe that the longer route taken here has the advantage of clarifying the interpretation of the neutral stability curves for the related bending problems discussed in (**7**, **10**). Following Haughton (**10**), we plot in Fig. 5 the critical azimuthal stretch λ_1 on the inner face as a

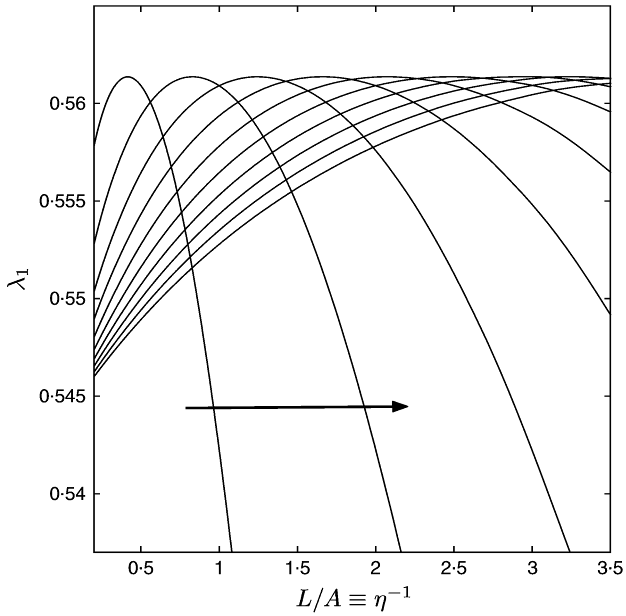

Fig. 5 A plot of critical values of $\lambda_1 \equiv \lambda(\rho_1)$ against undeformed length L/A for mode numbers $1 \leqslant n \leqslant 10$ (see also Fig. 5 in (**10**)). The arrow indicates the direction of increasing n

function of the inverse aspect ratio $\eta^{-1} = L/A$, for $1 \leqslant n \leqslant 10$. Although a different formulation of the eigenproblem was used in that work—without recourse to any potential function—the results we show are the same (as they should be since the height of the rubber block was fairly large, $H/A = 10$). The only exception is the unusual feature seen in that paper for $n = 1$, which we did not find with our model.

The response curves shown in Fig. 5 are reminiscent of similar situations encountered in the buckling of thin-walled structures (for example, (**25**)). For those particular problems, n represents the number of half waves of the instability pattern and plots like the one shown above can be used to infer the wavelength of the buckling pattern from the knowledge of some aspect ratio (some recent work in that direction can be found in (**1** to **3**)). In the present context, such extrapolations appear to provide misleading information for the obvious reason that n is not the true mode number. There are, however, some asymptotic features that can be gleaned from the plots in Fig. 5 and this is explained next.

Triantafyllidis (**7**) and Gent and Cho (**15**) suggested that the inner face of the bent block wrinkles due to a surface instability phenomenon. Biot (**24**, **26**) showed that if a semi-infinite neo-Hookean solid is compressed in plane strain, it will undergo a surface instability when $\lambda_1 \simeq 0{\cdot}544$ or, more precisely, when λ_1 is the positive root of the cubic

$$x^3 + x^2 + x - 1 = 0 \tag{3.1}$$

(cf. also Flavin (**27**)). This expectation is anticipated by the results of Fig. 3 in the limit $\eta \to \infty$ and corresponds to $m \to \infty$ (see the lower-right asymptotic value of the thick curve). On the other hand, the same conclusion is not so obvious from Fig. 5 because it proves to be very difficult to approach the limit $\eta^{-1} \to 0$ much beyond of what is already shown there. Indeed, the differential equation (2.12) becomes very stiff due to the presence of a BL near $\rho = \rho_1$, as it is explained in section 4.2. Nevertheless, based on the above discussion it is appropriate to conjecture that the left end points of all curves in that plot will tend towards Biot's surface instability threshold as $\eta^{-1} \to 0$; further remarks on related stability problems where this crops up are included in (**28**).

4. Stress concentration for $n \gg 1$

The mathematical structure of the boundary-value problem derived in section 2 is akin to a number of interesting situations investigated recently in the literature by Fu *et al.* (**18**, **29**) and Haughton and Chen (**19**). Broadly speaking, these authors encountered a particular occurrence of turning points (for example, (**30**)) or repeated roots in the characteristic equations associated with bifurcation analyses for everted cylindrical/spherical shells. It was stated that such special points could aid in detecting sites of high-stress concentration within elastic solids. Furthermore, in view of the recent work on edge buckling of thin films (**1** to **3**), it would appear reasonable to conclude that Fu's observation might go a long way towards explaining the localised behaviour seen in Fig. 4. That this is not true we are going to see in section 4.2, but before we pursue those issues it is important to gain an understanding of the relevance of WKB techniques in the present context. According to the previous interpretation of the parameters $\eta \equiv A/L$ and n (defined in (2.11)), the bifurcation of a thick rubber block ($\eta \gg 1$) can be understood by taking $\eta = 1$ and allowing $n \gg 1$.

4.1 *WKB approach*

The WKB method is a simple and efficient tool for dealing with variable-coefficient linear differential equations containing certain small or large parameters. We exploit the presence of $\mu \equiv \pi n \gg 1$ in our eigenproblem to describe the dependence of ω_0 (or λ_1) on this large parameter.

A WKB solution of (2.12) is sought in the form

$$\Phi(\rho) = Y(\rho) \exp\left(\mu \int_{\rho_1}^{\rho} S(\xi) d\xi\right), \tag{4.1a}$$

$$Y(\rho) = Y_0(\rho) + \frac{1}{\mu} Y_1(\rho) + \frac{1}{\mu^2} Y_2(\rho) + \cdots, \tag{4.1b}$$

where $S \equiv S(\rho)$ is one of the roots of the characteristic equation

$$S^4 - \left(\omega_0^2 \rho^2 + \frac{1}{\omega_0^2 \rho^2}\right) S^2 + 1 = 0$$

and $Y_j(\rho)$ ($j = 0, 1, \ldots$) are functions that are to be determined sequentially by substituting the ansatz (4.1) into (2.12), and then solving the differential equations obtained by setting to zero the coefficients of like powers of μ. The above bi-quadratic has four real roots, labelled

$$S_1^{(\pm)}(\rho) := \pm \omega_0 \rho, \quad S_2^{(\pm)}(\rho) := \pm \frac{1}{\omega_0 \rho},$$

and they lead to a set of linearly independent (approximate) solutions for (2.12). Given our experience with the direct numerical simulations of section 3, it is expected that only the exponentials corresponding to $S_{1,2}^{(-)}(\rho)$ need to be used in order to capture the through-thickness localised behaviour. We shall employ the superscripts '1' and '2' to identify quantities associated with these characteristic exponents in (4.1).

The determinantal equation that follows by imposing the boundary conditions (2.15) at $\rho = \rho_1$ on the WKB solutions $\Phi^{(1)}$ and $\Phi^{(2)}$ has the form

$$U_1(\rho_1)V_2(\rho_1) - U_2(\rho_1)V_1(\rho_1) = 0, \tag{4.2}$$

where

$$U_j(\rho) := \Phi^{(j)'''} - \mu^2 \left(\omega_0^2\rho^2 + \frac{2}{\omega_0^2\rho^2}\right)\Phi^{(j)'} + \frac{\mu^2}{\rho}\left(\omega_0^2\rho^2 + \frac{2}{\omega_0^2\rho^2}\right)\Phi^{(j)}, \tag{4.3}$$

$$V_j(\rho) := \Phi^{(j)''} - \frac{1}{\rho}\Phi^{(j)'} + \frac{\mu^2}{\omega_0^2\rho^2}\Phi^{(j)}, \quad j = 1, 2. \tag{4.4}$$

When calculating $\Phi^{(j)}$ $(j = 1, 2)$, terms of order $\mathcal{O}(\mu^{-2})$ and higher in the ansatz (4.1b) will be ignored. These solutions are fixed by routinely solving a series of non-homogeneous linear differential equations (the so-called 'transport equations'). Without loss of generality, the various multiplicative and additive constants in the expressions of those functions can be chosen to be unity and, respectively, zero; after some algebra,

$$Y_0^{(1)}(\rho) = \frac{\rho}{(1-\omega_0^4\rho^4)^{1/2}}, \quad Y_1^{(1)}(\rho) = -\frac{5\omega_0^8\rho^8 + 10\omega_0^4\rho^4 - 3}{4\omega_0\rho^2(1-\omega_0^4\rho^4)^2}Y_0^{(1)}(\rho),$$

$$Y_0^{(2)}(\rho) = \frac{\rho^2}{(1-\omega_0^4\rho^4)^{1/2}}, \quad Y_1^{(2)}(\rho) = \frac{3\omega_0(\omega_0^4\rho^4 + 1)}{2(1-\omega_0^4\rho^4)^2}Y_0^{(2)}(\rho),$$

and thus,

$$\Phi^{(j)}(\rho) \simeq \left\{Y_0^{(j)}(\rho) + \frac{1}{\mu}Y_1^{(j)}(\rho)\right\}\exp\left(\mu\int_{\rho_1}^{\rho} S_j^{(-)}(\xi)d\xi\right), \quad j = 1, 2. \tag{4.5}$$

It must be noted that $Y_i^{(j)}$ $(i = 0, 1;\ j = 1, 2)$ become singular when $\rho = \overline{\rho} \equiv \omega_0^{-1} \in (\rho_1, \rho_2)$; in the language of differential equations, this represents a (multiple) turning point of the differential equation (2.12). Such points are usually defined as those values of the independent variable for which some of the roots of the characteristic equation coalesce. For this particular example, both $S_1^{(+)}(\overline{\rho}) = S_2^{(+)}(\overline{\rho})$ and $S_1^{(-)}(\overline{\rho}) = S_2^{(-)}(\overline{\rho})$, that is, two pairs of roots merge. Strictly speaking, the validity of the above formulae for $Y_i^{(j)}$ $(i = 0, 1;\ j = 1, 2)$ requires $|\rho - \overline{\rho}| \gg \mu^{-1/2}$. Although $\overline{\rho}$ depends on the unknown eigenvalue, our numerical experiments suggest that the turning point remains confined to the central part of the interval (ρ_1, ρ_2). The connection problem across the turning point can be easily solved following the detailed analysis of Fu and Lin (**18**) but plays no role in the sequel.

On making use of (4.5) into (4.2), we are able to expand the determinantal equation in decreasing integral powers of $\mu \gg 1$,

$$\Gamma_0(\lambda_1) + \Gamma_1(\omega_0, \lambda_1)\frac{1}{\mu} + \Gamma_2(\omega_0, \lambda_1)\frac{1}{\mu^2} + \cdots = 0, \tag{4.6}$$

with

$$\Gamma_0(z) := 8z^2(z^2+1)^2(z^3 - z^2 + z + 1)(z^3 + z^2 + z - 1),$$

$$\Gamma_1(\omega_0, z) := 2\omega_0(4z^{12} + 15z^{10} + 23z^8 + 8z^4 - 7z^2 - 3)$$

and

$$\Gamma_2(\omega_0, z) := \frac{\omega_0^2}{(z^2+1)^2(z^2-1)^4}(6z^{22} - 18z^{20} - 37z^{18} - 477z^{16} - 1118z^{14} \\ - 930z^{12} - 600z^{10} - 4z^8 - 120z^6 - 140z^4 + 45z^2 + 33).$$

The solution of (4.6) yields approximations for both the critical bending angle ω_0 and the principal stretch λ_1. For the sake of brevity, we record only the final results here:

$$\omega_0 = \overline{\Omega}_0 + \frac{\overline{\Omega}_1}{\mu} + \frac{\overline{\Omega}_2}{\mu^2} + \cdots, \tag{4.7}$$

$$\overline{\Omega}_0 = 0{\cdot}771844, \quad \overline{\Omega}_1 = -1{\cdot}305565, \quad \overline{\Omega}_2 = 15{\cdot}39664$$

and

$$\lambda_1 = \Lambda_0 + \frac{\Lambda_1}{\mu} + \frac{\Lambda_2}{\mu^2} + \cdots, \tag{4.8}$$

$$\Lambda_0 = 0{\cdot}543689, \quad \Lambda_1 = 0{\cdot}385922, \quad \Lambda_2 = -4{\cdot}184333.$$

As expected, $\Lambda_0 \simeq 0{\cdot}544$ represents the critical value of the principal stretch for the surface instability of a compressed neo-Hookean half-space (cf. (**24**, **26**)); the next-order corrections in formula (4.8) account for the finite size of the rubber block. To assess the usefulness of the two asymptotic results (4.7) and (4.8), a set of comparisons with direct numerical simulations is recorded in Table 1. The agreement is excellent for both ω_0 and λ_1; in particular, we find that the relative accuracy (RA) associated with ω_0 ranges between 1·4% ($n = 7$) and 0·8% ($n = 20$). The approximation of λ_1 is even better, for RA is at most 0·4% ($n = 7$) in all cases considered.

The WKB analysis has the advantage of producing a robust approximation for ω_0 (or λ_1) with minimum effort. However, the presence of the turning point is worrisome because it tends to obscure the true nature of the localised behaviour exhibited by (2.12). It is not immediately clear whether such behaviour has anything to do with the turning point, and thus a change of tack is imperative. Section 4.2 shows that conventional BL techniques are better suited for understanding the underlying mathematical structure responsible for the scenario depicted in Fig. 4. The details of that particular approach are now highlighted.

Table 1 Comparisons between direct numerical simulations of the eigenproblem (2.12), (2.15) and the asymptotic results recorded in the formulae (4.7), (4.8). The bending angle and the azimuthal stretch on the inner boundary associated with the former set of values are denoted by ω_0^{num} and, respectively, λ_1^{num}. The corresponding asymptotic quantities are identified below as ω_0^{asy} and λ_1^{asy}

n	ω_0^{num}	ω_0^{asy}	λ_1^{num}	λ_1^{asy}
7	0·744313103	0·733652725	0·555301084	0·552585690
8	0·744272309	0·736778030	0·554325988	0·552419947
9	0·744928414	0·739453964	0·553494699	0·552104104
10	0·745886633	0·741762924	0·552780068	0·551733662
11	0·746957132	0·743772049	0·552160229	0·551352710
12	0·748046186	0·745533828	0·551618218	0·550981720
13	0·749107553	0·747090530	0·551140475	0·550629796
14	0·750119338	0·748474960	0·550716526	0·550300415
15	0·751072409	0·749714126	0·550337796	0·549994245
16	0·751964384	0·750829238	0·549997574	0·549710574
17	0·752796399	0·751837997	0·549690282	0·549448050
18	0·753571374	0·752754745	0·549411416	0·549205075
19	0·754293016	0·753591537	0·549157200	0·548980000
20	0·754965302	0·754358139	0·548924583	0·548771235

4.2 *BL analysis*

To begin, we introduce the stretched variable $X = \mathcal{O}(1)$ such that $\rho = \rho_1 + X\mu^{-1}$ and look for solutions of (2.12) with

$$W(X) = W_0(X) + W_1(X)\frac{1}{\mu} + W_2(X)\frac{1}{\mu^2} + \cdots, \tag{4.9a}$$

$$\omega_0 = \Omega_0 + \frac{\Omega_1}{\mu} + \frac{\Omega_2}{\mu^2} + \cdots, \tag{4.9b}$$

$$\rho_1 = \Delta_0 + \frac{\Delta_1}{\mu} + \frac{\Delta_2}{\mu^2} + \cdots. \tag{4.9c}$$

Although (4.9b) and (4.9c) are not independent, it helps to expand ρ_1 in the form suggested here. Of course, when solving the governing equations for the coefficients $W_j(X)$ ($j = 0, 1, \ldots$) one has to remember formula (2.13) and replace the Δ_k's with their expressions in terms of the Ω_j ($j = 0, 1, \ldots, k$).

On substituting (4.9) into (2.12), we find a hierarchy of differential equations

$$\mathcal{L}_{\text{BL}}[W_k] = \sum_{i=0}^{k-1}\sum_{j=1}^{3} A_{ij}^{(k)} \frac{d^j W_i}{dX^j} \quad (k \geqslant 0), \tag{4.10}$$

in which

$$\mathcal{L}_{\mathrm{B\,L}} := \frac{d^4}{dX^4} - \left(\zeta_0^2 + \frac{1}{\zeta_0^2}\right)\frac{d^2}{dX^2} + 1$$

is the BL differential operator and $\zeta_0 := \Delta_0\Omega_0$. The quantities $A_{ij}^{(k)} \equiv A_{ij}^{(k)}(X)$ will be introduced as we go along, with the convention that $A_{ij}^{(0)} \equiv 0$. In contrast to the WKB analysis, the general solution of each one of the equations in (4.10) is trivially found, for $\mathcal{L}_{\mathrm{BL}}$ has constant coefficients.

Equations (4.10) are solved subject to two types of boundary conditions. The first set is obtained from (2.15) with the help of the ansatz (4.9) and can be cast in the general form

$$\mathcal{H}_1[W_k] = \sum_{i=0}^{k-1}\sum_{j=0,1} B_{ij}^{(k)}\frac{d^j W_i}{dX^j}, \quad \text{for } X = 0, \tag{4.11a}$$

$$\mathcal{H}_2[W_k] = \sum_{i=0}^{k-1}\sum_{j=0,1} C_{ij}^{(k)}\frac{d^j W_i}{dX^j}, \quad \text{for } X = 0, \tag{4.11b}$$

where

$$\mathcal{H}_1 := \frac{d^3}{dX^3} - \left(\zeta_0^2 + \frac{2}{\zeta_0^2}\right)\frac{d}{dX} \quad \text{and} \quad \mathcal{H}_2 := \frac{d^2}{dX^2} + \frac{1}{\zeta_0^2};$$

the remark made for the $A_{ij}^{(k)}$s applies to the boundary coefficients $B_{ij}^{(k)}$ and $C_{ij}^{(k)}$ as well.

The second set of boundary conditions is motivated by the numerical experiments illustrated in Fig. 4 and it involves the requirement that

$$\frac{d^j W_i}{dX^j} \to 0 \quad \text{as } X \to \infty, \tag{4.12}$$

for $i \geqslant 0$, $j = 0, \ldots, 3$. It is also worth pointing out that the solution of (2.12) is exponentially small in the outer layer (cf.section 4.1), so that (4.12) can be viewed as matching conditions between the inner and the outer solutions.

The leading-order problem for $W_0(X)$ is homogeneous and consists of the differential equation (4.10) for $k = 0$, together with the boundary conditions (4.11). Rejecting the exponentially growing contributions and imposing the normalisation condition $W_0(X = 0) = 1$, it follows that

$$W_0(X) = \frac{2}{1 - \zeta_0^4}\exp(-\zeta_0 X) - \frac{1 + \zeta_0^4}{1 - \zeta_0^4}\exp\left(-\frac{X}{\zeta_0}\right). \tag{4.13}$$

When this function is substituted into the boundary conditions, one obtains an algebraic equation

$$\zeta_0^8 + 2\zeta_0^4 - 4\zeta_0^2 + 1 = 0,$$

whose left-hand side can be factorised in terms of (3.1) and two other polynomials which have no positive roots different from unity. It remains that $\zeta_0 \simeq 0{\cdot}543689$, a value identical to Λ_0 found in section 4.1; the same turns out to be true for Ω_0 in (4.9b) and, respectively, $\overline{\Omega}_0$ in (4.7).

The next-order problem corresponds to taking $k = 1$ in (4.10) and (4.11). The coefficients that appear in these equations are

$$A_{01}^{(1)} := \frac{1}{\Delta_0 \zeta_0^2}(\zeta_0^4 - 3), \qquad A_{02}^{(1)} := \frac{2}{\zeta_0^3}(\Delta_0 \boldsymbol{\Omega}_1 + \Delta_1 \boldsymbol{\Omega}_0 + \boldsymbol{\Omega}_0 X)(\zeta_0^4 - 1), \quad A_{03}^{(1)} := \frac{2}{\Delta_0},$$

$$B_{00}^{(1)} := -\frac{\boldsymbol{\Omega}_0}{\zeta_0^3}(\zeta_0^4 + 2), \qquad B_{01}^{(1)} := \frac{2}{\zeta_0^3}(\Delta_0 \boldsymbol{\Omega}_1 + \Delta_1 \boldsymbol{\Omega}_0)(\zeta_0^4 - 2),$$

$$C_{00}^{(1)} := \frac{2}{\zeta_0^3}(\Delta_0 \boldsymbol{\Omega}_1 + \Delta_1 \boldsymbol{\Omega}_0), \quad C_{01}^{(1)} := \frac{1}{2} A_{03}^{(1)}.$$

The first-order correction $\boldsymbol{\Omega}_1$ in the expansion (4.9b) of the eigenvalue ω_0 is recovered by enforcing the Fredholm solvability condition on the non-homogeneous equation satisfied by $W_1(X)$. The task is simplified by the observation that the homogeneous problem for $W_0(X)$ is self-adjoint. Standard calculations show that the constraint mentioned amounts to

$$C_{01}^{(1)} \left\{ \frac{dW_0}{dX}(0) \right\}^2 + \{C_{00}^{(1)} - B_{01}^{(1)}\} W_0(0) \frac{dW_0}{dX}(0) - B_{00}^{(1)} \{W_0(0)\}^2$$

$$= \int_0^\infty W_0(\xi) \sum_{j=1}^{3} A_{0j}^{(1)} \frac{d^j W_0}{dX^j}(\xi) d\xi. \tag{4.14}$$

Note that the integral on the right-hand side in (4.14) is evaluated analytically, and thus the solvability condition will reduce to a linear equation in $\boldsymbol{\Omega}_1$. The solution $\boldsymbol{\Omega}_1 \simeq -1{\cdot}305562$ is, for all practical purposes, identical to the WKB result obtained earlier.

The pattern of the BL approach for the pure bending problem is now clear: at each step, one has to impose a solvability condition for finding $\boldsymbol{\Omega}_j$ that features in (4.9b), and then solve (exactly) a non-homogeneous fourth-order boundary-value problem to get $W_j(X)$. The algebraic manipulations become increasingly unwieldy as we move to further orders, but symbolic algebra packages help considerably. We have imposed the solvability condition for the W_2-problem and found that the value of $\boldsymbol{\Omega}_2$ predicted agrees with $\overline{\boldsymbol{\Omega}}_2$ to within five significant digits; for completeness, the coefficients needed to set up that problem are recorded below:

$$A_{11}^{(2)} := \frac{\boldsymbol{\Omega}_0}{\zeta_0^3}(\zeta_0^4 - 3), \quad A_{12}^{(2)} := A_{02}^{(1)}, \quad A_{13}^{(2)} := A_{03}^{(1)},$$

$$A_{01}^{(2)} := \frac{1}{\zeta_0^4}[\boldsymbol{\Omega}_0^2 (X + \Delta_1)(\zeta_0^4 + 9) + 2\boldsymbol{\Omega}_1(\zeta_0^4 + 3)\zeta_0], \quad A_{03}^{(2)} := -\frac{2}{\Delta_0^2}(X + \Delta_1),$$

$$A_{02}^{(2)} := \frac{1}{\zeta_0^4}\{2\Delta_0 \boldsymbol{\Omega}_0 (\Delta_0 \boldsymbol{\Omega}_2 + \Delta_2 \boldsymbol{\Omega}_0)(\zeta_0^4 - 1) + [\boldsymbol{\Omega}_0^2 (X + \Delta_1)^2 + \Delta_0^2 \boldsymbol{\Omega}_1^2](\zeta_0^4 + 3)$$
$$+ 4\boldsymbol{\Omega}_1 (X + \Delta_1)(\zeta_0^4 + 1)\zeta_0 - 3\boldsymbol{\Omega}_0^2 \zeta_0^2\},$$

$$B_{00}^{(2)} := -\frac{1}{\zeta_0^4}[\Delta_1 \boldsymbol{\Omega}_0^2 (\zeta_0^4 - 6) + 2\boldsymbol{\Omega}_1(\zeta_0^4 - 2)\zeta_0],$$

$$B_{01}^{(2)} := \frac{1}{\zeta_0^4}[2(\Delta_0 \boldsymbol{\Omega}_2 + \Delta_2 \boldsymbol{\Omega}_0)(\zeta_0^4 - 2)\zeta_0 + (\Delta_0^2 \boldsymbol{\Omega}_1^2 + \Delta_1^2 \boldsymbol{\Omega}_0^2)(\zeta_0^4 + 6) + 4\Delta_1 \boldsymbol{\Omega}_1 (\zeta_0^4 + 2)\zeta_0],$$

$$B_{10}^{(2)} := B_{00}^{(1)}, \quad B_{11}^{(2)} := B_{01}^{(1)},$$

$$C_{00}^{(2)} = -\frac{1}{\zeta_0^4}[3(\Delta_0^2\Omega_1^2 + \Delta_1^2\Omega_0^2) - 2\zeta_0(\Omega_0\Delta_2 + \Delta_0\Omega_2 - 2\Delta_1\Omega_1)],$$

$$C_{01}^{(2)} = -\frac{\Delta_1}{\Delta_0^2}, \quad C_{10}^{(2)} = C_{00}^{(1)}, \quad C_{11}^{(2)} = C_{01}^{(1)}.$$

It might appear that our BL approach is a by-product of adopting the simple neo-Hookean form for the constitutive response of the bulk material. However, this impression is only apparent, for when choosing a strain energy function of the form

$$W(\lambda_r, \lambda_\theta) \propto (\lambda_r^q + \lambda_\theta^q - 2), \quad (q > 1), \tag{4.15}$$

the same mathematical structure persists. The corresponding analysis mirrors very closely that for the present case and hence is omitted. By no means should this give the impression that the constitutive behaviour is unimportant. As demonstrated in a recent study by Goriely *et al.* (**28**), the topology of the neutral stability curves for an inflated hyperelastic spherical shell depends on the material non-linearity, but in the present context this would amount to considering expressions more general than the power law (4.15).

5. Concluding remarks

We have re-examined the bifurcations in cylindrical bending of a thick rubber block under the assumption of plane strain deformation. The constitutive behaviour was taken to be that of a neo-Hookean incompressible solid, the reason for this being twofold: we wanted to (a) exclude any material instabilities and (b) simplify our equations as much as possible. The outcome turned out to be a fourth-order eigenproblem with variable coefficients. Direct numerical simulations and singular perturbation methods were employed to unravel the origins of the rippling pattern triggered on the compressed face of the block, when the bending angle is sufficiently large. It has been shown in section 3 that previous investigators (**7**, **10**, **15**) misinterpreted the definition of the so-called 'mode number' and thus made a number of inaccurate statements. In particular, we want to reiterate here that blocks of large, but finite, thickness will always experience an Euler-type buckling instability with a well-defined number of ripples. It is only in the (theoretical) limit of an infinitely thick block that one finds the degenerate surface instability. Our results deal with the neo-Hookean material, but it is believed that the above statement remains valid in other cases as well. Provided that material instabilities are excluded, it seems unlikely that a different choice of constitutive law would have qualitative repercussions on the main conclusions of the present investigation.

Our work has also demonstrated that the use of WKB methods in the context of incremental elasticity is unnecessary and even misleading. The multiple turning point featuring in the present eigenproblem has little to do with the tendency of the rippling deformation to confine itself near the curved inner surface of the block. Interestingly, a simple-minded BL analysis was able to expose the nature of the localisation in an almost trivial way. In spite of the original complexity of the problem, we found that if the rubber block is sufficiently thick, its possible bifurcations from the cylindrical configuration are governed by constant-coefficient differential equations—easily solved in closed form. This has important overall implications since preliminary calculations indicate that the problems taken up in (**11**, **18**, **19**, **29**) are amenable to a similar BL analysis. The details of those investigations will be the subject of a forthcoming work (**31**).

Acknowledgements

This research is funded by an International Joint Project awarded by the Royal Society of London (UK) and the Centre National de la Recherche Scientifique (France). The authors acknowledge with gratitude the support of these organisations. Thanks are also due to Professor Raymond Ogden and Dr David Haughton (University of Glasgow) for enlightening discussions concerning the difference between the constitutive behaviour used in (**7**) and (**10**). Both authors thank the referees for their constructive remarks that have helped tighten the presentation.

References

1. C. D. Coman and A. P. Bassom, On the wrinkling of a pre-stressed annular thin film in tension, *J. Mech. Phys. Solids* **55** (2007) 1601–1617.
2. C. D. Coman and A. P. Bassom, Boundary layers and stress concentration in the circular shearing of annular thin films, *Proc. R. Soc.* A **463** (2007) 3037–3053.
3. C. D. Coman and D. M. Haughton, Localised wrinkling instabilities in radially stretched annular thin films, *Acta Mech.* **185** (2006) 179–200.
4. S. Kyriakides and E. Corona, *Mechanics of Offshore Pipelines: Buckling and Collapse* (Elsevier Science, Oxford 2007).
5. P. Seide and V. I. Weingarten, On the buckling of circular cylindrical shells under pure bending, *ASME J. Appl. Mech.* **28** (1961) 112–116.
6. P. E. Tovstik and A. L. Smirnov, *Asymptotic Methods in the Buckling Theory of Elastic Shells* (World Scientific, Singapore 2000).
7. N. Triantafyllidis, Bifurcation phenomena in pure bending, *J. Mech. Phys. Solids* **28** (1980) 221–245.
8. R. Hill and J. W. Hutchinson, Bifurcation phenomena in the plane tension test, *ibid.* **23** (1975) 239–264.
9. N. J. B. Young, Bifurcation phenomena in the plane compression test, *ibid.* **24** (1976) 77–91.
10. D. M. Haughton, Flexure and compression of incompressible elastic plates, *Int. J. Engng Sci.* **37** (1999) 1693–1708.
11. G. Dryburgh and R. W. Ogden, Bifurcation of an elastic surface-coated incompressible isotropic elastic block subject to bending, *Z. Angew. Math. Phys.* **50** (1999) 822–838.
12. M. Aron and Y. Wang, On deformations with constant modified stretches describing the bending of rectangular blocks, *Q. Jl Mech. Appl. Math.* **48** (1995) 375–387.
13. M. Aron and Y. Wang, Remarks concerning the flexure of a compressible nonlinearly elastic rectangular block, *J. Elast.* **40** (1955) 99–106.
14. O. T. Bruhns, H. Xiao and A. Meyers, Finite bending of a rectangular block of an elastic Hencky material, *ibid.* **66** (2002) 237–256.
15. A. N. Gent and I. S. Cho, Surface instabilities in compressed or bent rubber blocks, *Rubber Chem. Technol.* **72** (1999) 253–262.
16. R. W. Penn and E. A. Kearsley, The scaling law for finite torsion of elastic cylinders, *Trans. Soc. Rheol.* **20** (1976) 227–238.
17. G. P. MacSithigh, Necessary conditions at the boundary for minimisers in incompressible finite elasticity, *J. Elast.* **81** (2005) 217–269.
18. Y. B. Fu and Y. P. Lin, A WKB analysis of the buckling of an everted neo-Hookean cylindrical tube, *Math. Mech. Solids* **7** (2002) 483–501.

19. D. M. Haughton and Y.-C. Chen, Asymptotic bifurcation results for the eversion of elastic shells, *Z. Angew. Math. Phys.* **54** (2002) 191–211.
20. A. E. Green and W. Zerna, *Theoretical Elasticity* (Clarendon Press, Oxford 1960).
21. R. W. Ogden, *Non-Linear Elastic Deformations* (Dover, New York 1997).
22. R. S. Rivlin, Large elastic deformations of isotropic materials V: the problem of flexure, *Proc. R. Soc.* A **195** (1949) 463–473.
23. H. G. Allen, *Analysis and Design of Structural Sandwich Panels* (Pergamon Press, Oxford 1969).
24. M. A. Biot, *Mechanics of Incremental Deformations* (Wiley, New York 1965).
25. N. A. Alfutov, *Stability of Elastic Structures* (Springer, Berlin 2000).
26. M. A. Biot, Surface instability of rubber in compression, *Appl. Sci. Res.* **A12** (1963) 168–182.
27. J. N. Flavin, Surface waves in pre-stressed Mooney material, *Q. Jl Mech. Appl. Math.* **16** (1963) 441–449.
28. A. Goriely, M. Destrade and M. Ben Amar, Instabilities in elastomers and soft tissues, *ibid.* **59** (2006) 615–630.
29. Y. B. Fu and M. S. Pour, WKB method with repeated roots and its application to the buckling analysis of an everted cylindrical tube, *SIAM J. Appl. Math.* **62** (2002) 1856–1871.
30. C. M. Bender and S. A. Orszag, *Advanced Mathematical Methods for Scientists and Engineers* (Springer, New York 1999).
31. C. D. Coman, Boundary layers and bifurcation problems in finite elasticity, to appear.